Acta Crystallographica Section D
Biological Crystallography
ISSN 0907-4449

Structure of *Escherichia coli* fragment TR_2C from calmodulin to 1.7 Å resolution

Lise-Lotte Olsson and Lennart Sjölin*

Department of Inorganic Chemistry and the Center for Structural Biology, Göteborg University, SE-412 96 Göteborg, Sweden

Correspondence e-mail: lennart@inoc.chalmers.se

Received 28 November 2000
Accepted 19 February 2001

PDB Reference: calmodulin TR_2C fragment, 1fw4.

Fragment TR_2C is the C-terminal part of the calcium-binding protein calmodulin, including residues 78–148. The crystal structure of TR_2C was solved by molecular replacement and refined to a conventional R value of 21.8% (R_{free} = 22.0%), using all data in the resolution range 20.0–1.7 Å. This study shows that the secondary structure of TR_2C, a pair of EF-hand motifs with two calcium-binding sites, is similar to the corresponding motifs in intact calmodulin. However, it also indicates that the N-terminus of helix *E* is closer to the C-terminus of helix *H* in TR_2C than in the intact protein and that the loop connecting the EF-hands shows different conformations in the two structures. The crystal structure of TR_2C was further found to be similar to the set of NMR structures of this fragment, although some pronounced differences exist.

1. Introduction

The calcium-binding protein calmodulin (CaM), which is ubiquitous in eukaryotic systems, combines with and modulates the activity of a wide variety of enzymes (Manalan & Klee, 1984). It has a broad distribution within the cell and throughout different tissues and species (Finn *et al.*, 1995). CaM is a small heat-stable acidic protein which consists of 148 amino-acid residues. The crystallographic structure reported for CaM (Babu *et al.*, 1988) is far from being optimally packed and exhibits a characteristic dumbbell shape with one pair of EF-hands in each lobe. The structure is more compact in solution and the dynamics of its long connecting helix is very important in the process of enzyme activation (Persechini & Kretsinger, 1988; Zhang *et al.*, 1995). Crystal structures of the parent protein CaM bound to, for example, TFP (Cook *et al.*, 1994; Vandonselaar *et al.*, 1994) show that the tertiary structure of CaM changes from an elongated dumbbell to a compact globular form. Recently, the CaM structure from *Paramecium tetraurelia* was solved to 1.0 Å resolution by Wilson & Brunger (2000). This high-resolution structure allowed a detailed analysis of the structural disorder, which indicated a high degree of functional flexibility in the protein.

In the presence of Ca^{2+} ions CaM can be cleaved by trypsin, mainly after Lys77. Subsequently, two fragments TR_1C (residues 1–77) and TR_2C (residues 78–148) are formed. It has previously been shown that both fragments TR_1C and TR_2C bind calcium in a similar manner as the complete CaM molecule (Thulin *et al.*, 1984). The two tryptic fragments are also able to bind target enzymes but not to activate them (Newton *et al.*, 1983; Minowa *et al.*, 1988). It has further been suggested that TR_1C and TR_2C show conformations similar to

© 2001 International Union of Crystallography
Printed in Denmark – all rights reserved

those in the intact CaM molecule (Ikura *et al.*, 1985; Forsén *et al.*, 1986, 1991; Dalgarno *et al.*, 1984).

Recently, the solution structures of the apo and Ca^{2+} forms of the TR_2C domain of CaM were solved (Finn *et al.*, 1995; Kuboniwa *et al.*, 1995). They have essentially equal secondary structure, but Ca^{2+} binding causes major rearrangements of the secondary-structure elements.

The previously presented crystal structure of TR_2C to 3.6 Å resolution (Sjölin *et al.*, 1990) is to be replaced by the current structure to 1.7 Å resolution. The availability of the crystal structure of TR_2C to this higher resolution will be a complement to the previous NMR structures.

2. Experimental

2.1. Crystallization

The fragment TR_2C was expressed in *Escherichia coli* and purified as described by Finn *et al.* (1995). Crystals were grown by vapour diffusion employing the hanging-drop technique at room temperature. Each droplet was formed by mixing 2 µl of protein solution (88 mg ml^{-1}) with 2 µl of reservoir solution consisting of 15% PEG 4000 as the precipitating agent, 40 m*M* sodium acetate buffer solution pH 4.6 and 70 m*M* $CaCl_2$. In 2 d, octahedral crystals of approximately 1.3 × 0.6 × 0.6 mm were grown. The TR_2C crystals used for data collection crystallized in the tetragonal space group $I4_1$, with unit-cell parameters $a = b = 37.8$, $c = 99.8$ Å and $Z = 1$. The volume per unit mass V_M is 2.3 $Å^3$ Da^{-1}, which corresponds to a solvent content of 45% (Matthews, 1968).

2.2. Data collection

Data were collected to 1.7 Å resolution on a MAR-II imaging-plate system mounted on a Rigaku rotating-anode X-ray generator. The exposure time was 240 s for each of the 90 frames of 1° oscillation. This data set was not complete at low resolution and hence it was scaled to a second 3.4 Å low-resolution data set collected at BL711 at the MAX-lab II synchrotron in Lund, Sweden, also on an image-plate detector. The exposure time was only 1 s per degree. Both data sets were collected at room temperature and were processed and scaled with *DENZO* and *SCALEPACK* (Otwinowski & Minor, 1997), resulting in 7694 unique reflections. The overall temperature factor obtained from the Wilson plot is 32.2 $Å^2$ (Wilson, 1949). The statistics of the final data set are summarized in Table 1.

2.3. Structure solution and refinement

Phases for the TR_2C model were obtained by the molecular-replacement technique (Lattman, 1985) using *AMoRe* (Navaza, 1994). Residues 85–144 from the C-terminal part of the 1.7 Å CaM structure (Chattopadhyaya *et al.*, 1992; referred to as the 1.7 Å CaM structure) were used as the search model. The structure was originally solved for a 2.5 Å resolution data set with unit-cell parameters $a = b = 37.4$, $c = 100.1$ Å (unpublished results). Residues 84–143 of this structure were then used as the model for the new 1.7 Å data set. Even though the unit-cell parameters of the new crystal were close to those of the previously solved structure, it was not possible to solve the structure by simply placing the old model into the new cell. Instead, *AMoRe* was used again, which gave distinct rotation- and translation-function peaks for 15.0–3.0 Å data. The fitting program was used to optimize the rotation angles and the translational parameters; the top peak had a correlation coefficient of 0.82 and an *R* value of 30.4%. 4.7% of the data were excluded from all refinement for calculation of a free *R* value (Brünger, 1992). The model was then subjected to rigid-body refinement using *REFMAC* (Murshudov *et al.*, 1997) from the *CCP*4 package (Collaborative Computational Project, Number 4, 1994) for data in the resolution range 15.0–2.4 Å and an R_{free} of 36.5% and an R_{cryst} of 32.1% were obtained. With subsequent positional and individual temperature-factor refinement including all data to 1.7 Å and insertion of two well defined calcium ions the R_{free} was reduced to 34.6% (R_{cryst} = 30.8%). The model was improved by simulated annealing (Brünger *et al.*, 1990) using *X-PLOR* (Brünger *et al.*, 1987), alternating cycles of manual rebuilding using the computer graphics package *O* (Jones *et al.*, 1991) and maximum-likelihood refinement with *REFMAC*. After insertion of the N-terminal amino acids 81–83, the C-terminal residues 144 and 145 as well as 38 water molecules, R_{free} dropped to 27.5% (R_{cryst} = 23.5%).

In an attempt to better account for the bulk solvent, the refinement program was changed to *CNS* (Adams *et al.*, 1997) while keeping the same set of test reflections. This altered R_{free}

Table 1
Data and refinement statistics.

Values in parentheses refer to the highest resolution shell, 1.78–1.70 Å.

Data	
Resolution (Å)	20.0–1.7
Completeness (%)	99.9 (99.3)
Multiplicity	4.0 (3.2)
R_{merge} (%)	7.3 (36.7)
$\langle I/\sigma(I)\rangle$	13.3 (3.0)
$I/\sigma(I) > 3$ (%)	73.6 (28.0)
Model	
No. of residues	65
No. of protein atoms	534
No. of calcium ions	2
No. of solvent molecules	40
Missing residues	
N-terminal	78–80
C-terminal	146–148
Refinement	
R_{free} (%)	22.0 (43.4)
R_{cryst} (%)	21.8 (39.0)
Average ADP† ($Å^2$)	
Protein	45.2
Main chain	41.8
Side chain	48.5
Solvent molecules	49.6
Stereochemistry	
R.m.s.d. in bonds (Å)	0.0127
R.m.s.d. in angles (°)	1.59
R.m.s.d. ADP for bonded atoms† ($Å^2$)	
Main chain	3.87
Side chain	5.74

† ADP = atomic displacement parameter.

and R_{cryst} to 24.6 and 24.5%, respectively, without additional adjustments. Further refinement with *CNS* combined with rebuilding using *O* and inclusion of two additional water molecules gave a final R_{free} of 22.0% and an R_{cryst} of 21.8%. The electron density for the N- and C-terminal residues 78–80 and 146–148, respectively, is too weak for inclusion of these residues in the model. Water molecules were inserted in the model if they showed well defined σ_A-weighted $F_o - F_c$ and $2F_o - F_c$ electron-density maps and if they could make hydrogen bonds not longer than 3.2 Å to other atoms. Only two water molecules are included with hydrogen bonds in the range 3.4–3.5 Å. All water occupancies were set to unity. Calculated composite omit maps (*CNS*) agree well with the model. All reflections with $F > 0\sigma(F)$ were included in the refinement. The statistics of the refinement results are summarized in Table 1.

The average real-space correlation coefficient (Jones *et al.*, 1991) is 0.88 (Fig. 1). In the Ramachandran plot (Ramakrishnan & Ramachandran, 1965) from *PROCHECK* (Laskowski *et al.*, 1993), 96.6% of all non-glycine residues lie in the most favoured regions and 3.4% (Asp93 and Asp129) are found in the additional allowed regions. These two residues are both located at the first positions in the calcium-binding loops.

3. Results and discussion

3.1. General structure

The secondary structure of TR_2C is similar to the C-terminal half of the native CaM structure, as can be seen from the superposed plot viewed in Fig. 2. Helix *E* (residues 82–92), the third calcium-binding loop (according to CaM numbering) and helix *F* (102–111) form the third EF-hand. The fourth EF-hand is made up by helix *G* (118–128), the fourth calcium-binding loop and helix *H* (138–145). These two similar motifs are connected by a non-calcium-binding loop.

3.2. Solvent and crystal packing

All but three of the 40 identified solvent molecules are in the first hydration shell, making at least one hydrogen bond to the protein; 14 of these waters also bridge symmetry-related protein molecules either directly or *via* a second water molecule. There is only one hydrogen bond less than 2.5 Å within the structure, between a well defined water molecule and Glu120 OE1 (2.4 Å). No water molecules are found in the hydrophobic cleft.

There are 11 direct crystal contacts shorter than 3.3 Å between TR_2C and three different symmetry-related protein molecules. One of the interactions is with helix *G* from a neighbouring molecule, with hydrogen bonds between Arg90 and Glu123 and between Glu87 and Glu127. Asp93, at the first position of the third calcium-binding loop, also forms a hydrogen bond to Glu123. Asp93 and Arg90 also interact with a second neighbouring symmetry molecule. Arg90 hydrogen bonds to Gly113 and Lys115, which also hydrogen bonds to Asp93. A third crystal contact, related by a crystallographic twofold axis, is particularly close and particularly involves residues Met109, Glu114 and Gln143 and their symmetry mates. Glu114 OE2 is very close (1.8 Å) to the symmetry-

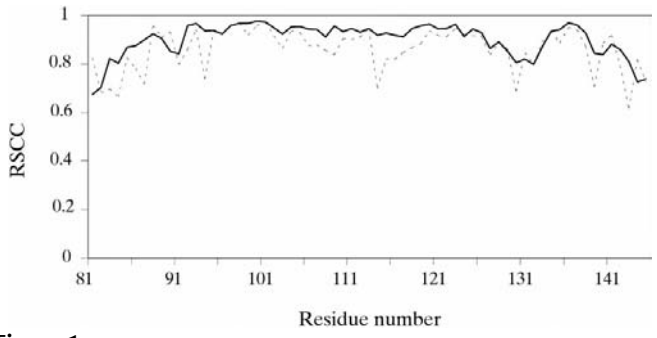

Figure 1
Average real-space correlation coefficients (RSCCs) for the final $2F_o - F_c$ map. Solid line, main chain; dashed line, side chain.

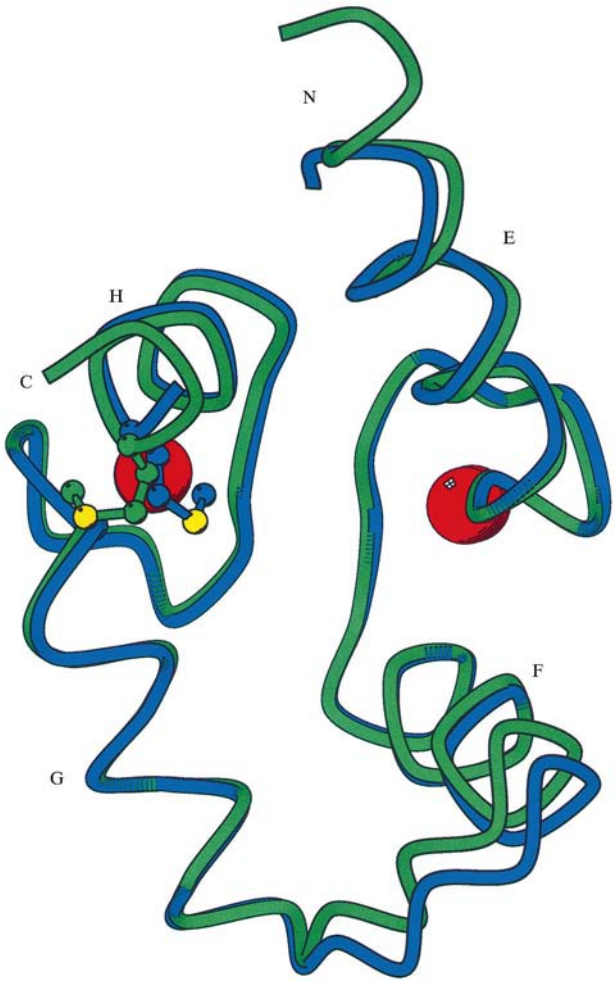

Figure 2
Schematic presentation of TR_2C (blue) superposed on the C-terminal half of the 1.7 Å CaM structure (green). The C^{α} atoms of residues 84–109 and 118–144 were used in the superposition. The calcium ions are represented by red spheres. Met144 is in ball-and-stick representation, with the S atoms in yellow. Helices *E*–*H* are labelled and N and C represent the amino and carboxyl termini, respectively. Figs. 2 and 4 were generated with the program *MOLSCRIPT* (Kraulis, 1991).

related Glu114 OE2. This is the closest contact in the model, but the density for this residue indicates that the two neighbouring side chains have slightly different conformations, which has not been accounted for in the model. Between these two molecules there are also hydrogen bonds between Glu114 and Glu120, and between Glu84 and Lys94.

3.3. Calcium coordination

TR_2C contains two Ca^{2+}-binding sites and in this crystal structure both of them are occupied by a calcium ion. The calcium-binding domains have the EF-hand conformation (helix–loop–helix) typical for many calcium-binding proteins (for a review, see Kawasaki & Kretsinger, 1994). The first calcium ion is coordinated to amino acids in the segment that includes residues 93–104 and the second one to amino acids in the segment including residues 129–140. Both segments are located on the surface of the molecule, with the calcium ions separated by 11.6 Å (11.5 Å in CaM). The calcium ions exhibit the same type of sevenfold coordination as in the parent CaM structure and the arrangement of the ligands can be described as a distorted pentagonal bipyramid. Typical calcium–oxygen distances are found in the fragment: between 2.19 and 2.55 Å in the first loop, and between 2.16 and 2.54 Å in the second loop. These two Ca^{2+}-binding loops form a short antiparallel β-strand held together by two hydrogen bonds between Ile100 and Val136, both at the eighth position in the two loops. The β-strand is also stabilized by two bridging water molecules, between Gly98 O and Tyr138 N, and between Ala102 N and Gly134 O, also observed in the 1.7 Å CaM structure. In the TR_2C structure the side chain of Asn137 has been rotated around the CB—CG bond compared with the 1.7 Å CaM structure, in order to change the positions of atoms OD1 and ND2. This change suggests well defined hydrogen bonds between Asn137 OD1 and the main-chain amides of residues Glu139 and Glu140.

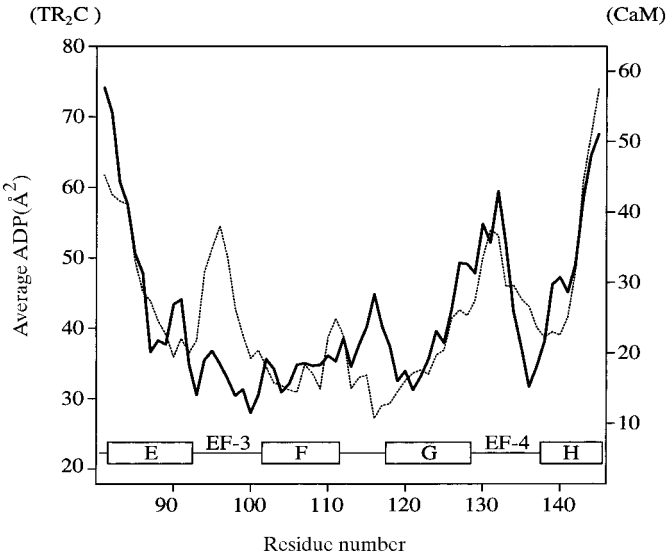

Figure 3
ADPs for the main chains of TR_2C (solid line) and the C-terminal half of the 1.7 Å CaM structure (dashed line). Their respective ADP mean values are aligned. The positions of helices *E*–*H* and the EF hands EF-3 and EF-4 are indicated.

3.4. Hydrophobic surfaces

There is a large exposed hydrophobic cleft in TR_2C formed by 14 hydrophobic side chains. This cleft is in general similar to the cleft in the C-terminal half of CaM, with only minor differences between the two structures for most of the residues. One of the major changes, however, is that the side chain of Met144 extends out over the opening of the cleft instead of pointing away from the cleft as in the 1.7 Å CaM structure. This gives a more than 4 Å difference in the position of 144 CE when TR_2C and CaM are superposed (Fig. 2). The two hydrophobic recognition sites for receptors in native CaM have four methionines each and the different sulfur pattern in TR_2C could influence the receptor binding to the fragment. A second major change is the side chain of Leu116, which is more buried in the cleft in TR_2C than it is in CaM.

3.5. Comparison of TR_2C with calmodulin

If the C^{α} positions of TR_2C are compared with the corresponding positions in the 1.7 Å CaM structure the r.m.s. deviations are small (Table 2). The non-calcium-binding loop has an r.m.s. deviation of 0.59 Å and the remaining deviations are in the range 0.12–0.29 Å for separate secondary-structure elements. For the entire fragment the deviation is higher (0.66 Å). If the non-EF-hand turn is excluded, the r.m.s. deviation for the rest of the fragment is somewhat lower (0.46 Å). This means that the angles between the helices and loops are different in TR_2C and CaM, giving a slightly different tertiary structure. The angle between helix *E* and the third calcium-binding loop differs by approximately 6° in TR_2C and CaM. This brings the N-terminal part of helix *E* in TR_2C 1 Å closer to the C-terminal part of helix *H* and TR_2C becomes more compact. Since conformational changes are important for the mechanism of action for EF-hand-containing proteins, this small change or difference between the structures may reflect another possible conformation utilized in the activation process. Another explanation could

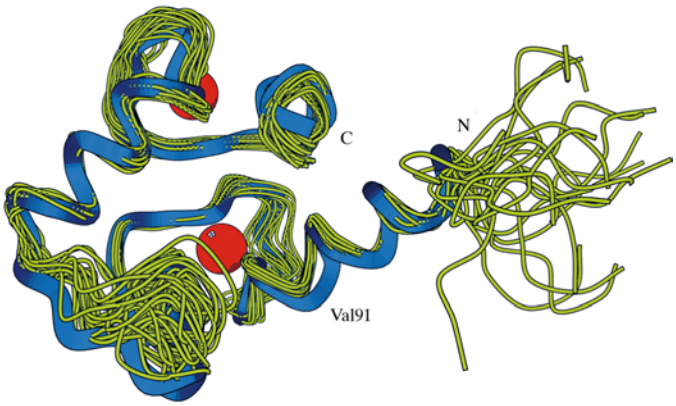

Figure 4
The X-ray structure of TR_2C (thick blue line) superposed on the family of 20 TR_2C NMR structures (thin green lines). Calcium ions are represented by red spheres. The position of Val91 is indicated.

Table 2
R.m.s. deviations between the C^{α} atoms in TR_2C and CaM (Chattopadhyaya *et al.*, 1992) in the specified residue ranges.

The N- and C-termini (81–83 and 145) are omitted.

	Residues	R.m.s.d. (Å)
Helix *E*	84–92	0.29
Third Ca^{2+} loop	93–104	0.16
Helix *F*†	102–109	0.14
Turn†	110–117	0.59
Helix *G*	118–128	0.26
Fourth Ca^{2+} loop	129–140	0.15
Helix *H*	138–144	0.12
Fragment	84–144	0.66
Fragment parts‡	84–109, 118–144	0.47

† For these calculations, residues 110 and 111 of helix *F* are included in the non-calcium-binding loop region because of their high r.m.s.d. values. ‡ The turn connecting the EF-hands is excluded.

be attributed to crystal packing in the vicinity of the third calcium loop and helix *E*. The non EF-hand turn is involved in close crystal contacts in the fragment as well as in CaM, which also affects the side chains in this loop. The direction of side chain Lys115 is slightly different in the two structures, Leu116 in the hydrophobic cleft has a different conformation as already described and the double conformations reported for Asp118 in the 1.7 Å CaM structure are not observed in the fragment.

The average atomic displacement parameter (ADP) for the main-chain atoms of TR_2C is 41.8 $Å^2$ (σ = 10.9) and the corresponding value for residues 81–145 of the 1.7 Å CaM structure is 25.3 $Å^2$ (σ = 10.0), giving a 16.5 $Å^2$ higher mean value for TR_2C. It is interesting to note that the standard deviations are about the same for the two structures. The parameters are compared in Fig. 3, which shows high values for the N- and C-termini for both structures. For TR_2C the ADP for the N-terminus is approximately 32 $Å^2$ higher than the mean value and for CaM it is only approximately 20 $Å^2$ above the mean value. This reflects the higher flexibility of helix *E* after the cleavage in the central helix connecting the two lobes in CaM. Ser81 is no longer in α-helical conformation and the side chains of residues 82–84 have weak electron density. This can be compared with the CaM structure of Babu *et al.* (1988), where residues 79–81 show significant deviation from ideal α-helical geometry and the ADPs in that region are among the highest in the structure. In helix *E* of TR_2C some of the side chains (Glu82, Glu83, Arg86, Glu87 and Arg90) have significantly different conformations compared with CaM. The short hydrogen bond between the side chains of Glu82 and Arg86, reported by Babu *et al.* (1988) and Chattopadhyaya *et al.* (1992) as being 2.2 and 2.1 Å, respectively, is completely lost in the TR_2C structure. The distance between Arg86 NH1 and Glu82 OE2 becomes as long as 11.2 Å. For Glu87, two alternate conformations can be observed.

For the C-terminus the previously determined ADP mean value is exceeded by approximately 25 $Å^2$ for TR_2C and by approximately 32 $Å^2$ for CaM. Furthermore, in the third calcium-binding loop the highest ADP for TR_2C is ~5 $Å^2$ lower than the mean value, but for CaM it is as much as 13 $Å^2$ higher. This region is stabilized by crystal contacts in the fragment, which could influence the movement of these atoms. For the non-EF-hand turn in TR_2C the highest mean ADP is slightly above the overall mean (~3 $Å^2$), but for CaM it is approximately 14 $Å^2$ lower than the mean value.

The beginning of the fourth calcium-binding loop has similarly high deviations from the mean values for both structures, but the end of the loop is found to be more stable in the fragment than in the intact protein, with a minimum in TR_2C found for Val136. Ile100 in the third calcium-binding loop has the lowest minimum in the fragment and together with Val136 it forms the short stabilizing β-strand between the calcium-binding loops. Corresponding minima are not found for CaM.

At the surface of the protein there are some additional side chains with major differences. Arg106 has a more relaxed conformation in TR_2C than it has in CaM, where it is involved in crystal packing. Glu119 is close to symmetry-related molecules in both structures, which gives two distinct conformations. In CaM Glu139 is close to a neighbouring CaM molecule and is different in TR_2C.

3.6. Comparison of the X-ray structure of TR_2C with the Ca^{2+} NMR TR_2C structures

In Fig. 4, the X-ray structure of TR_2C is superposed on the Ca^{2+} NMR structures of TR_2C (Finn *et al.*, 1995). If only the C^{α} atoms are considered, the X-ray structure is, in general, well represented by the the family of NMR structures. Residues 90–92 at the C-terminal end of helix *E*, however, do not coincide at all with any of the NMR structures, although the NMR structures show low r.m.s. deviations in this area. The X-ray structures of TR_2C and CaM are similar for these residues, but they both have crystal packing interactions in this area.

For the backbones of the calcium-binding loops the r.m.s. deviations are small for the set of NMR structures. For the side chains the deviations are large and the arrangement of calcium ligands is not clear, since the positions of the calcium ions are not determined in the NMR structures. The crystal structure of TR_2C, however, confirms that the calcium coordination in the fragment is conserved compared with intact CaM. This is important since many experiments on binding of calcium to the fragment have been performed.

For the non-EF-hand turn (residues 109–117) the X-ray structure is not close to the mean of the set of NMR structures but is partly outside. In the NMR structures there are rather few constraints and subsequently high r.m.s. deviations within the family. In the X-ray structure on the other hand, this loop is involved in crystal packing. The deviations could thus be explained by the different methods, but they may also reflect a property of the polypeptide chain which may in turn be relevant to function. In the recent 1.0 Å resolution CaM structure by Wilson & Brunger (2000) it was clearly demonstrated using TLS and multiconformer analysis that certain forms of CaM are less structurally distinct than previously

believed. These findings are in good agreement with the indications found in our analysis.

We thank Eva Thulin and Sture Forsén for providing recombinant fragment TR_2C and for helpful and stimulating discussions. The use of the BL711 beamline (MAX-lab II, Lund, Sweden) is also gratefully acknowledged as well as AstraZeneca for providing excellent data-collection facilities. This work was supported by grants from the Swedish Natural Science Research Council.

References

Adams, P. D., Pannu, N. S., Read, R. J. & Brünger, A. T. (1997). *Proc. Natl Acad. Sci. USA*, **94**, 5018–5023.
Babu, Y. S., Bugg, C. E. & Cook, W. J. (1988). *J. Mol. Biol.* **204**, 191–204.
Brünger, A. T. (1992). *Nature (London)*, **355**, 472–475.
Brünger, A. T., Krukowski, A. & Erickson, J. (1990). *Acta Cryst.* A**46**, 585–593.
Brünger, A. T., Kuriyan, J. & Karplus, M. (1987). *Science*, **235**, 458–460.
Chattopadhyaya, R., Meador, W. E., Means, A. R. & Quiocho, F. A. (1992). *J. Mol. Biol.* **228**, 1177–1192.
Collaborative Computational Project, Number 4 (1994). *Acta Cryst.* D**50**, 760–763.
Cook, W. J., Walter, L. J. & Walter, M. R. (1994). *Biochemistry*, **33**, 15259–15265.
Dalgarno, D. C., Klevit, R. E., Levine, B. A., Scott, G. M. M., Williams, R. J. P., Gergely, J., Grabarek, Z., Leavis, P. C., Grand, R. J. A. & Drabikowski, W. (1984). *Biochim. Biophys. Acta*, **791**, 164–172.
Finn, B. E., Evenäs, J., Drakenberg, T., Waltho, J. P., Thulin, E. & Forsén, S. (1995). *Nature Struct. Biol.* **2**, 777–783.
Forsén, S., Linse, S., Drakenberg, T., Kördel, J., Akke, M., Sellers, P., Johansson, C., Thulin, E., Andersson, I. & Brodin, P. (1991). *Ciba Found. Symp.* **161**, 222–236.
Forsén, S., Vogel, H. J. & Drakenberg, T. (1986). *Calcium and Cell Function*, Vol. 6, edited by E. Cheung, pp. 113–157. San Diego: Academic Press.
Ikura, M., Minowa, O. & Hikichi, K. (1985). *Biochemistry*, **24**, 4264–4269.
Jones, T. A., Zou, J. Y., Cowan, S. W. & Kjeldgaard, M. (1991). *Acta Cryst.* A**47**, 110–119.
Kawasaki, H. & Kretsinger, R. H. (1994). *Protein Profile*, **1**, 343–517.
Kraulis, P. J. (1991). *J. Appl. Cryst.* **24**, 946–950.
Kuboniwa, H., Tjandra, N., Grzesiek, S., Ren, H., Klee, C. B. & Bax, A. (1995). *Nature Struct. Biol.* **9**, 768–776.
Laskowski, R. A., MacArthur, M. W., Moss, D. S. & Thornton, J. M. (1993). *J. Appl. Cryst.* **26**, 283–291.
Lattman, E. (1985). *Methods Enzymol.* **115**, 55–57.
Manalan, A. S. & Klee, C. B. (1984). *Adv. Cyclic Nucleotide Protein Phosphorylation Res.* **18**, 227–278.
Matthews, B. W. (1968). *J. Mol. Biol.* **33**, 491–497.
Minowa, O., Yazawa, M., Sobue, K., Ito, K. & Yagi, K. (1988). *J. Biochem. (Tokyo)*, **103**, 531–536.
Murshudov, G. N., Vagin, A. A. & Dodson, E. J. (1997). *Acta Cryst.* D**53**, 240–255.
Navaza, J. (1994). *Acta Cryst.* A**50**, 157–163.
Newton, D. L., Burke, T. R. Jr, Rice, K. C. & Klee, C. B. (1983). *Biochemistry*, **22**, 5472–5476.
Otwinowski, Z. & Minor, W. (1997). *Methods Enzymol.* **276**, 307–326.
Persechini, A. & Kretsinger, R. (1988). *J. Biol. Chem.* **263**, 12175–12178.
Ramakrishnan, C. & Ramachandran, G. N. (1965). *Biophys. J.* **5**, 909–933.
Sjölin, L., Svensson, L. A., Prince, E. & Sundell, S. (1990). *Acta Cryst.* B**35**, 117–121.
Thulin, E., Andersson A., Drakenberg, T., Forsén, S. & Vogel, H. G. (1984). *Biochemistry* **23**, 1862–1870.
Vandonselaar, M., Hickie, R. A., Quail, J. W. & Delbaere, L. T. J. (1994). *Nature Struct. Biol.* **1**, 795–801.
Wilson, A. J. C. (1949). *Acta Cryst.* **2**, 318–320.
Wilson, M. A. & Brunger, A. T. (2000). *J. Mol. Biol.* **301**, 1237–1256.
Zhang, M., Tanaka, T. & Ikura, M. (1995). *Nature Struct. Biol.* **2**, 758–767.